

Identification of Griffiths-like phase and its evolution in Cr substituted pyrochlore iridates $Y_2Ir_2O_7$

Vinod Kumar Dwivedi^{1,2,*}

¹Materials Science Programme, Indian Institute of Technology Kanpur, Kanpur 208016, India

²Department of Physics, Indian Institute of Science, Bengaluru 560012, India

We report the Griffiths phase (GP)-like state along with cluster-glass-like state in geometrically frustrated antiferromagnetic Cr substituted $Y_2Ir_2O_7$ pyrochlore iridates. The strength of GP-like behaviour increases with substitution. Interestingly, isothermal remanent magnetization suggests the Ising-like interaction of spins in GP region. The GP-like state is not attributed to the structural disorder as substitution of Cr does not induces any structural change. Then the spin coupling between $Cr^{3+} \leftrightarrow Cr^{3+}$, $Ir^{4+} \leftrightarrow Ir^{4+}$, $Ir^{4+} \leftrightarrow Cr^{3+}$ and $Ir^{4+} \leftrightarrow Ir^{5+}$ leads the competition between antiferromagnetic and ferromagnetic correlations. It give rise to Ruderman-Kittel-Kasuya-Yosida (RKKY)-like interaction between Cr^{3+} local magnetic moments mediated by itinerant Ir conduction electrons, hence, as a result GP and cluster-glass-like states emerges.

I. INTRODUCTION

A spin glass (SG) is known as a randomly distributed mixed interacting bonds (antiferro and ferromagnetic) characterized by a collective freezing of the spins at a definite temperature T_{SG} below which a highly irreversible metastable frozen state appears without the usual magnetic long range ordering, where each and every spin reside in a frustrated state¹. Spin glasses show a phase transition from a high temperature paramagnetic (PM) state into low temperature glassy state with exponential relaxation of spins. Long back, it have been reported that low temperature magnetic state fuses into a state whose correlation functions follow non-exponential tails² due to the emergence of same un-frustrated clusters favour to the growth of Griffiths phase^{3,4} in the magnetization, sandwiched between the spin-glass and paramagnetic state.

The Griffiths phase (GP) was initially suggested for randomly diluted Ising ferromagnets, where only a tiny part of the lattice sites are filled with spins and remaining fractions are either empty or occupied with non-magnetic ions. Further, it has been shown that disorder suppresses the magnetic transition from its clean value of T^* (Griffiths temperature) to long-range magnetic ordering temperature T_C ³. GP is characterized by formation of magnetically ordered rare regions within the global paramagnetic (PM) matrix at $T_C < T < T^*$. Such a system contains sharp downturn at high temperature regime in inverse magnetic susceptibility $1/\chi$ vs T curve below T^* ⁵. The physics of GP is closely related to quenched disorder and competing interactions⁵⁻¹¹. In fact, GP behaviour have mostly been reported in the diluted ferromagnetic systems with positive value of Curie-Weiss (CW) temperature θ_{CW} , however, there are *very limited* experimental reports on GP exhibiting negative value of CW temperature θ_{CW} in antiferromagnetic (AFM) systems¹¹⁻¹⁵.

In pyrochlore iridates $R_2Ir_2O_7$ (R = Y, Bi, Rare earth elements), the interplay of spin-orbit coupling, electronic correlation and crystal electric field comparable at energy scales offer many emergent quantum phases¹⁶⁻²⁰, can be achieved by tuning the strength of relative energy scales via chemical substitution²¹⁻³⁰, reducing the particle sizes³¹⁻³⁵, lattice mismatch induced strain effects^{9,36} etc. Although, theoretically $Y_2Ir_2O_7$ (YIO) is expected to be a candidate of magnetic Weyl semimetal¹⁷ with all-in/all-out antiferromagnetic

(AFM) ground state. Moreover, neutron diffraction and inelastic scattering measurements of YIO powder sample^{37,38} does not show any sign of long-range magnetic ordering for small-moments of $Ir^{4+}(5d^5)$ within the measurement limit of instrument. However, these measurements do not rule out long-range magnetic order, but do put an upper limit for the Ir^{4+} ordered moment of $\sim 0.2 \mu_B/Ir$ (for a magnetic structure with wave vector $Q \neq 0$) or $\sim 0.5 \mu_B/Ir$ (for $Q = 0$) based on the structural refinements of neutron powder diffraction pattern. On the other hand, muon spin relaxation (μSR) is very sensitive to probe internal magnetic fields as a result of ordered magnetic moments or random fields that are static or fluctuating (of a few Gauss) with time due to its large gyromagnetic ratio. The zero field μSR measurements of YIO powder sample shows the appearance of spontaneous muon spin precessions below transition temperature confirms the long-range magnetic ordering³⁸⁻⁴¹. Recently, the glass-like state⁴² in YIO has also been reported, where the chemical doping of magnetic $Ru^{4+}(4d^4)$ ion²³, non-magnetic $Ti^{4+}(3d^0)$ ion²³ at magnetic $Ir^{4+}(5d^5)$ -site and the substitution of magnetic $Pr^{3+}(4f^2)$ for the non-magnetic $Y^{3+}(4d^0)$ -site²⁴ separately, enhances the magnetic relaxation rate. Moreover, it have also been shown that YIO exhibit weak ferromagnetic (FM) component along with a large AFM ground state^{19-21,29,30,43}. Despite these advances, a conclusive understanding of the precise nature of magnetic state is not yet fully established.

In this manuscript, we attempt to bridge the lacking by our latest finding by gradual substitution of magnetic ion $Cr^{3+}(3d^3)$ at $Ir^{4+}(5d^5)$ magnetic site in geometrically frustrated AFM pyrochlore iridates YIO, i.e. $Y_2Ir_{2-x}Cr_xO_7$ (YICO). We find that YIO shows GP along with the cluster-glass like state and these properties enhance on increasing the doping concentration. This substitution would produce following effects: (I) It would bring magnetic impurity in the Ir^{4+} sublattice, (II) It would alter the concentration of charge carrier which in turn change the $3d - 5d$ magnetic exchange interaction between the local Cr^{3+} moments (randomly distributed in the Ir-sublattice) and itinerant Ir^{4+} conduction electrons, (III) Since $Cr^{3+}(3d^3)$ have relatively larger strength of electronic correlation and low value of spin-orbit coupling compared to $Ir^{4+}(5d^5)$, the substitution will likely to induce disorder. Our results show the presence of magnetically ordered rare regions at $T_C < T < T^*$, support the for-

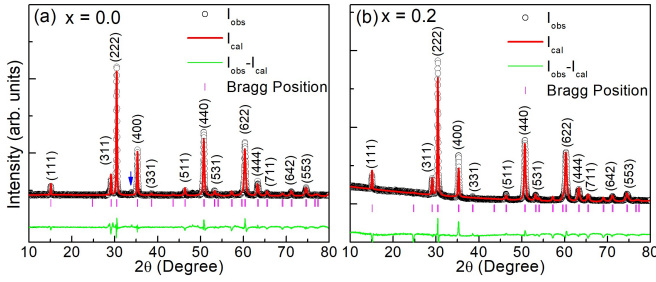


FIG. 1: Room temperature XRD pattern of (a) $x = 0.0$, and (b) $x = 0.2$ samples. Arrow represents Y_2O_3 parasitic phase.

mation GP-like state in YIO sample. The strength of magnetically ordered rare regions enhances as doping concentration of Cr increases. Interestingly, the nature of interacting spins in the GP regime founds to be Ising-like. In addition, the cluster glass-like state at low temperature is also observed.

II. EXPERIMENTAL METHOD

Polycrystalline samples of the YICO series ($x = 0.0, 0.05, 0.1, 0.2$) were synthesized using the conventional solid state reaction route following the protocols described elsewhere^{27,44}. High purity stoichiometric amount of starting materials Y_2O_3 , IrO_2 and Cr_2O_3 were mixed, ground, pelletized and heated in air at 1000 °C for 100 h, at 1050 °C for 200 h with several intermediate grinding with heating and cooling rate 3 °C/min. Room temperature powder x-ray diffraction (XRD) pattern were measured to check the structural phase formation of the samples using PANalytical XPert-PRO diffractometer with $Cu-K\alpha$ radiation ($\lambda = 1.54056 \text{ \AA}$). The x-ray photoelectron spectroscopy (XPS) measurements were recorded using a PHI 5000 Versa Probe II system with an energy resolution of 0.02 eV and step size 0.05 eV. dc magnetic measurements were performed between 2-350 K with a 14 T Quantum Design Physical Property Measurement System (PPMS) using vibrating sample magnetometry (VSM) mode. ac susceptibility measurement was carried out in a cryogenic S700X model Superconducting Quantum Interference Device (SQUID) magnetometer down to 5 K at frequencies 50 Hz and 1 kHz with an excitation field $H_{ac} = 0.1 \text{ Oe}$ and dc drive field $H_{dc} = 1000 \text{ Oe}$.

III. RESULTS AND DISCUSSION

The powder XRD patterns measured at room temperature of two representative samples $x = 0.0$ and 0.2 of YICO series are shown in Figs. 1a-b. The XRD pattern was analyzed by Rietveld refinement using the software FULLPROF, confirming the phase purity of the samples. Refinement shows a pyrochlore cubic crystal structure with $Fd\bar{3}m$ space group. For $x = 0.0$ sample, a small impurity phase of Y_2O_3 was detected in the sample shown by arrow in Fig. 1a which are in agreement with earlier literatures^{21,43}. For $x = 0.2$ sample, impurity

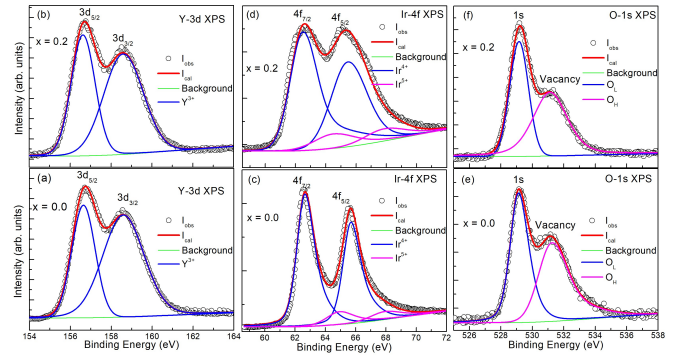


FIG. 2: Deconvoluted XPS spectra measured at room temperature of (a) Y-3d, (b) Ir-4f, and (c) O-1s of two representative samples $x = 0.0$ and 0.2 of the series YICO.

phase was not found. Y_2O_3 is diamagnetic in nature, hence it would not affect magnetic properties of the YICO series. The lattice parameter a , $Ir - O - Ir$ bond angle obtained from refinement for $x = 0.0$ and 0.2 samples are 10.16 \AA , 120° and 10.00 \AA , 108° , respectively. It suggests reduction of lattice constant and bond angle with substitution of Cr. Figure 2a-f display the XPS spectra of $x = 0.0$ and 0.2 samples. Y-3d XPS peaks shown in Fig. 2a-b show a single feature suggest the presence of Y^{3+} in both samples which is in agreement with earlier reports²⁶⁻²⁸. Figure 2c-d show deconvoluted Ir-4f XPS spectra which can be fitted with two sets of doublets related to the contribution from Ir^{4+} and Ir^{5+} which is in agreement with reports^{26-28,31,32}. We find that for $x = 0.2$ sample, the contribution from Ir^{5+} is increased, indicating co-presence of mixed oxidation states i.e., Ir^{4+} and Ir^{5+} . Further support of mixed valence states can also be seen in O-1s XPS spectra [Fig. 2e-f]. The peaks centered at binding energies 529 eV and 531.1 eV are associated as lower O_L and higher O_H binding energy peaks, respectively^{22,28,32}. The O-1s XPS spectra can be fitted with a set of doublet. We observed that the ratio of O_H and O_L is enhanced in $x = 0.2$ sample support the presence of mixed oxidation states of metal ion.

Temperature dependent magnetic susceptibility of two representative samples $x = 0.0$, and $x = 0.2$ of YICO series is shown in Fig. 3a. For the $x = 0.2$ sample, the ZFC magnetic susceptibility χ_{ZFC} increases gradually to a maximum around peak temperature T_f and then decreases monotonically as temperature reduces. A clear bifurcation between χ_{FC} and χ_{ZFC} curves at an irreversibility temperature T_{irr} is observed. The cusp in χ_{ZFC} vs T curve is more prominent for $x = 0.2$ compound ($\sim 50 \text{ K}$) as compared to $x = 0.0$ ($\sim 130 \text{ K}$, hardly visible in χ_{ZFC} vs T curve). The value of T_{irr} and T_f is given in Table I. A sharp rise in χ_{FC} and χ_{ZFC} curves below T_{irr} for both the samples suggest formation of FM clusters. Further, ferromagnetic transition temperature T_C can be estimated using the minima in χ_{ZFC} vs T curves, while maximum in χ_{ZFC} vs T curve indicates antiferromagnetic transition T_N . The determination of transition temperature is done following the protocol reported by the same author²⁷. The estimated values of T_C is given in Table I. Figure 3b shows real component of ac-susceptibility as

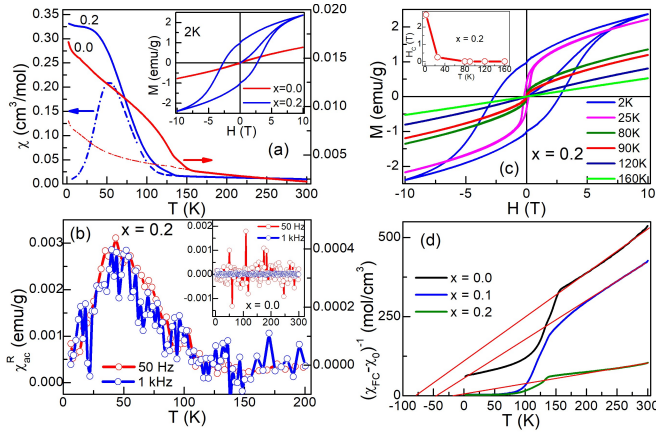


FIG. 3: (a) Variation of magnetic susceptibility ($\chi = M/H$) with temperature measured in the presence of $H = 1$ kOe following the zero-field-cooled (ZFC) and field-cooled (FC) protocol shown by short dash dot line and solid continuous line, respectively; inset shows magnetization as a function of magnetic field. (b) Real part of the ac susceptibility as a function of temperature measured at 50 Hz (right y-axis) and 1 kHz (left y-axis) for $x = 0.2$ sample; for $x = 0.0$, it is shown in inset, (c) Magnetic hysteresis loops of $x = 0.2$ sample measured at various temperatures; inset represents temperature dependent coercive field (H_C), (d) $(\chi_{FC} - \chi_0)^{-1}$ as a function of temperature; red solid continuous lines are a guide to the eyes.

a function of temperature for sample $x = 0.2$, suggests a well defined cusp at temperature ~ 50 K similar to freezing temperature T_f of χ_{ZFC} vs T curve. However, the quality of data is not good enough to fix any frequency dependence characterizing conventional spin glass-like feature. ac-susceptibility of $x = 0.0$ sample is shown in inset of Fig. 3b but the signal was very weak. Figure 3c shows the M vs H curves measured at several temperatures of $x = 0.2$ sample. The estimated value of H_C decreases monotonously as temperature increase [inset of Fig. 3c] and disappear above $T_C \sim 70$ K, however, it shows huge enhancement of H_C in the glassy state. It suggests evolution of glassy behaviour arises likely due to randomly arranged Cr ions in Ir-sublattice. Eventually, it is interesting to see that T_{irr} is far away from the T_f , and hysteresis in M vs H curves below T_C suggest formation of cluster glass (CG)-like behaviour⁴⁵ possibly due to the coexistence of mixed oxidation states of Ir. As a result, FM-PM transition arises due to FM super- and double exchange interactions via $\text{Ir}^{4+}-\text{O}^{2-}-\text{Cr}^{3+}$ or $\text{Ir}^{4+}-\text{O}^{2-}-\text{Ir}^{5+}$ path, respectively and glassy state at T_f because of $\text{Ir}^{4+}-\text{O}^{2-}-\text{Ir}^{4+}$ and $\text{Cr}^{3+}-\text{O}^{2-}-\text{Cr}^{3+}$ AFM couplings.

Further, the susceptibility of YICO series was analysed using the modified CW law, $\chi = \chi_0 + \frac{C}{T - \theta_{CW}}$; where C , θ_{CW} and χ_0 are the Curie constant, CW temperature, and temperature independent susceptibility, respectively. A fit using CW law well above T^* shown in the Fig. 3d give the best fitted values of important parameters are listed in Table I. The negative value of θ_{CW} for all the samples indicates antiferromagnetic correlations. The observations from a closer inspection of Fig. 3d are :- (1) non-linearity in the $(\chi_{FC} - \chi_0)^{-1}$ vs T curve at $T_{irr} < T < T^*$, likely due to the presence of strong

TABLE I: Parameters obtained from the magnetization data. FM transition temperature T_C is estimated from the minima in first derivative of χ vs T curve. H_C estimated from M(H) curve.

Sample	$x = 0.0$	$x = 0.05$	$x = 0.1$	$x = 0.2$
T^* (K)	230	240	240	245
T_{irr} (K)	160	155	145	140
T_C (K)	130	65	67	70
T_f (K)	130	46	48	50
$-\theta_{CW}$ (K)	75	70	40	10
μ_{eff}^{exp} ($\mu_B/\text{f.u.}$)	2.27	2.62	2.95	4.92
μ_{eff}^{theo} ($\mu_B/\text{f.u.}$)	1.73	2.57	2.68	2.9
H_C (T)	0.037	1.66	2.74	2.78
$GP_{Norm.} = \frac{T^* - T_C}{T_C}$	0.77	2.88	3.50	3.85

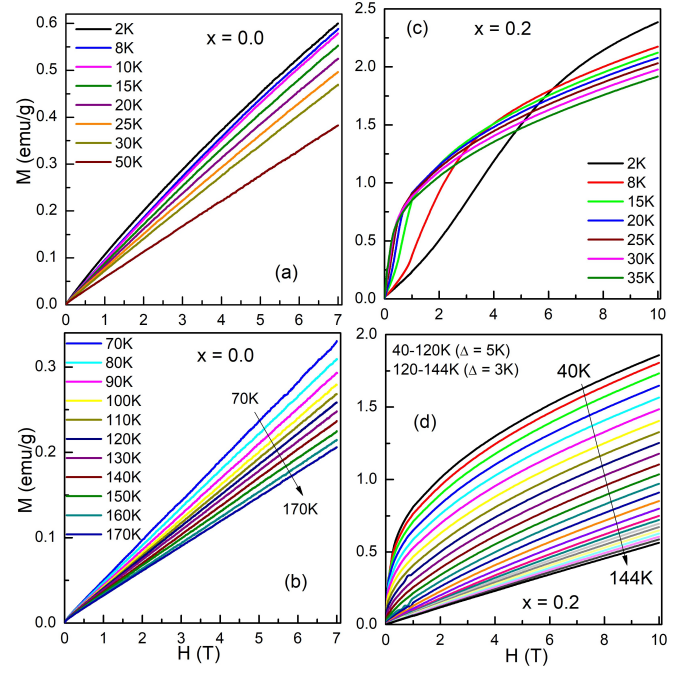


FIG. 4: Magnetic field dependence of virgin magnetization isotherms of $x = 0.0$ (a), (b) and $x = 0.2$ (c) and (d) samples.

crystal field. (2) $(\chi_{FC} - \chi_0)^{-1}$ vs T follows the CW law above T^* . (3) Larger value of experimental effective magnetic moments μ_{eff}^{exp} than theoretical μ_{eff}^{theo} . Theoretical effective magnetic moment can be estimated using the formula reported elsewhere^{26,29,30}, i.e., $\mu_{eff}^{theo} = \sqrt{(2-x)\mu_{Ir}^2 + x\mu_{Cr}^2}$, where μ_{Ir}^2 and μ_{Cr}^2 are the spin only contributed values of effective magnetic moment of Ir and Cr ions, respectively. The enhancement in μ_{eff}^{exp} as compared to μ_{eff}^{theo} suggests the formation of ferromagnetic clusters⁹. (4) A sharp downward deviation well below T^* . (5) Marginal upward deviation in $(\chi - \chi_0)^{-1}$ vs T curves from the ideal CW behaviour near T^* just before the start of downturn with lowering of temperature, similar to other systems^{8,46,47}. These observations suggest GP-like behaviour, i.e., formation of magnetically ordered rare regions in the global PM matrix at $T_C < T < T^*$.

Further, isothermal M vs H measurements at distinct tem-

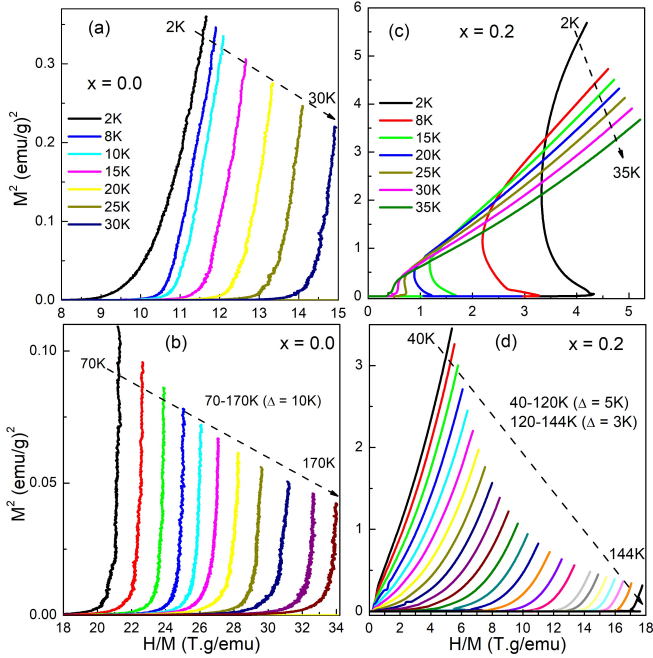


FIG. 5: Standard Arrott plots of two representative samples $x = 0.0$ (a), (b), and $x = 0.2$ (c), (d) of YICO series.

peratures have been carried out. All M vs H data were recorded in ZFC condition and before each successive magnetic isotherms, sample was heated above T^* to eliminate the magnetic history. This protocol is *important* for pyrochlore iridates to measure the M vs H isothermal magnetization. Figure 4a-d show the virgin isotherm magnetization curves for $x = 0.0$ (up to 7 T) and $x = 0.2$ (up to 10 T) samples at closely spaced temperatures. M vs H curves show monotonic enhancement with field without any sign of saturation for both the samples. The absolute values of M at 7 T and 2 K are estimated to be 0.6 emu/g ($0.07 \mu_B$) and 2.4 emu/g ($0.23 \mu_B$) for $x = 0.0$ and 0.2 samples, respectively. For sample $x = 0.0$, close inspection indicate a slight convex-like behaviour at low temperature [Fig. 4a], while linear nature [Fig. 4b] at high temperatures. On the other hand, sample $x = 0.2$ shows a crossover at low field up to 35 K [Fig. 4c]. Surprisingly, we do not find linear behaviour in M - H curve up to 170 K [Fig. 4d], suggest the presence of non-paramagnetic regime.

Further, to examine the strength and nature of the complex magnetic interactions, the conventional Arrott plots²⁸ (M^2 vs H/M) are shown in Fig. 5a-d. A negative intercept is observed for both the samples $x = 0.0$ and 0.2, suggest the absence of spontaneous magnetization. This information is important because long-range type AFM correlation possibly exhibit weak FM clusters. For $x = 0.2$ sample, the strength of negative intercept on M^2 axis decreases as compared to $x = 0.0$ with lowering of the temperature, suggests possibility of enhanced ferromagnetic signal. Interestingly, Arrott plot shows distorted “S”-like shape with negative curvature at low field (below 1T) shown in Fig. 5c, suggest the complex nature of field induced metamagnetic transition. In addition, non-straight M^2 curves with positive slope at low field and verti-

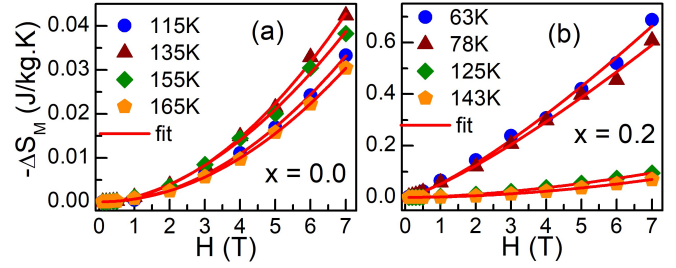


FIG. 6: $-\Delta S_M$ - H at different temperatures of (a) $x = 0.0$ and (b) $x = 0.2$ samples; red solid line represents H^n dependence.

cally at high field suggests the existence of short-range correlations in the proximity of AFM background in both samples.

In order to find further support for the GP behaviour, i.e., presence of magnetic clusters in the global paramagnetic matrix ranging $T_C < T < T^*$, the variation in magnetocaloric entropy change $\Delta S_M = \int_0^H (\partial M / \partial T) dH$ is estimated from M vs H isotherms. It has already been shown by the same author²⁷ that ΔS_M vs T measured at several fields exhibit the coexistence of conventional and inverse magnetocaloric effect (MCE) in Cr substituted YIO samples, emerging due to the coexistence and competition between the ferromagnetic and antiferromagnetic clusters. It is further analysed using the prediction of mean field theory, which suggests that ΔS_M vs H should follow the power law⁴⁸ behaviour $\Delta S_M \propto H^n$, where n is the local exponent of the entropy change. Further theory states that for an ideal FM system, the value of n should be 0.67 near T_C , ~ 1 well below T_C and 2 in the paramagnetic regime above T_C . We have fitted $-\Delta S_M$ vs H data using power law shown by red line in the Fig. 6a,b. The estimated values of n for the sample $x = 0.0$ turns out to be 1.88 (115 K), 1.92 (135 K), 1.95 (155 K), and 1.98 (165K). On the other hand for sample $x = 0.2$, the best fit value of n turns out to be 1.05 (63 K), 1.25 (77 K), 1.65 (125 K), and 1.85 (143 K). It is obvious that estimated value of n is less than 2 above T_C for both the samples, deviates from the ideal value of $n = 2$ above T_C for the paramagnetic regime. It suggests the presence of magnetic clusters above T_C in the global paramagnetic regime in YICO series. The lower values of n for the $x = 0.2$ sample also suggests the higher contribution of rare region in substituted samples compared to $x = 0.0$.

To elaborate the nature of probable GP, $\frac{1}{\chi}$ vs T graph were plotted at different fields. Figure 7a, b show a pronounced field dependent sharp and sudden downward deviation on approaching the magnetic transition from the high temperature PM region. The sharpness of downturn decreases with field and suppressed at higher field; although suppression of downturn with field is not systematic for $x = 0.0$ sample. Such behaviour is consistent with the characteristic of GP. Generally, magnetic systems exhibiting GP show:- (I) Sharp downward deviation of $\frac{1}{\chi}$ vs T curves from conventional CW behaviour below T^* , where the sharpness of this downturn decreases as H increases. (II) Overlapping of all the $\frac{1}{\chi}$ vs T curves measured at all field in the global PM regime above T^* . It is obvious that $\frac{1}{\chi}$ vs T curves measured at all applied magnetic

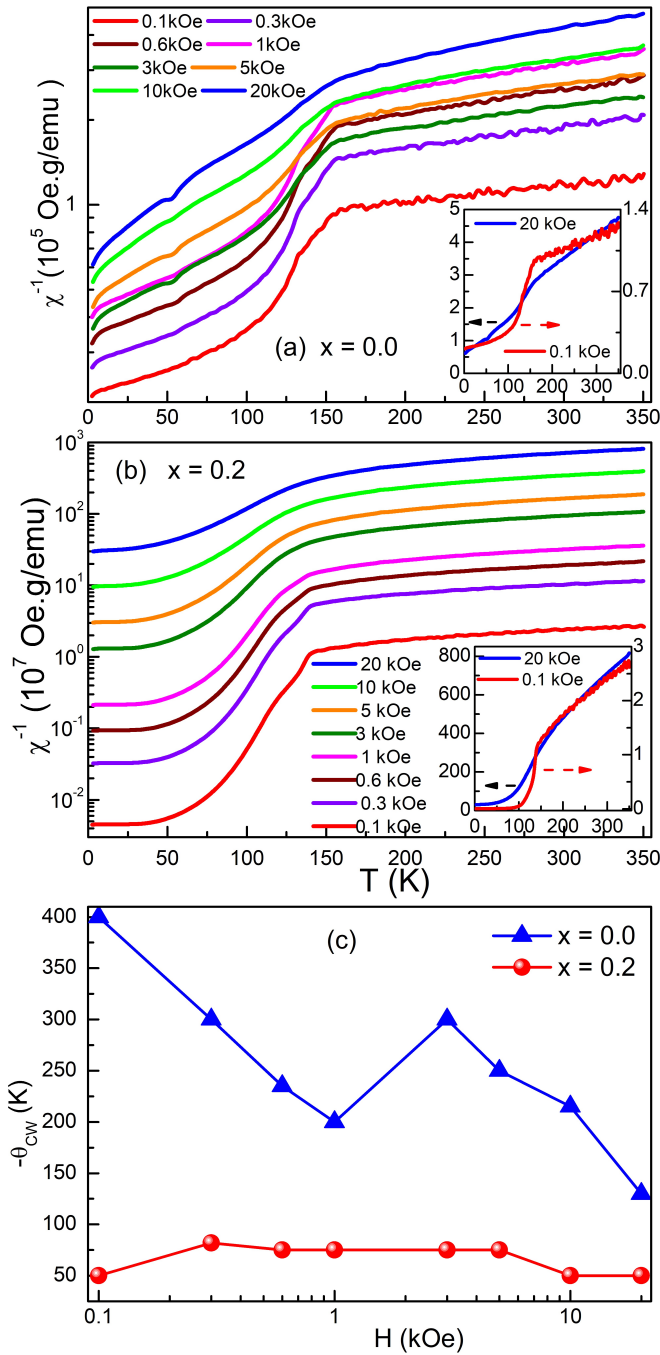


FIG. 7: Semi-log plot of χ^{-1} vs T for the samples (a) $x = 0.0$, (b) $x = 0.2$. Insets shows same at lowest and highest fields on linear scale. (c) Variation of $-\theta_{CW}$ with field.

field do not overlap in the global PM regime above T^* . This only means that the effect of external magnetic field is beyond the simple mean-field behavior. The variation of $-\theta_{CW}$ with H for both the samples is plotted in the Fig. 7c, indicates that the $-\theta_{CW}$ changes with field for the same sample. Moreover, it could be clusters or FM impurities, but also any other interaction that might be comparable with Zeeman energy at the given field. Thus, the GP-like state appear to be an inherent

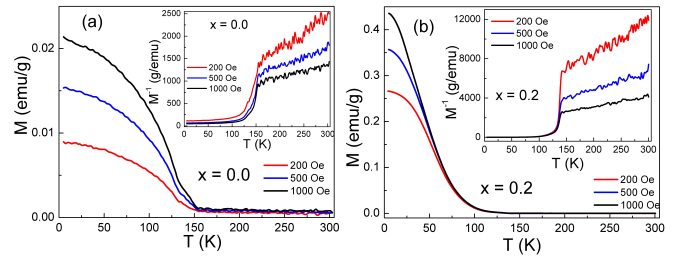


FIG. 8: Thermoremanent magnetization (TRM) as a function of temperature for (a) $x = 0.0$, and (b) $x = 0.2$ specimens; inset shows sharp downturn below T^* .

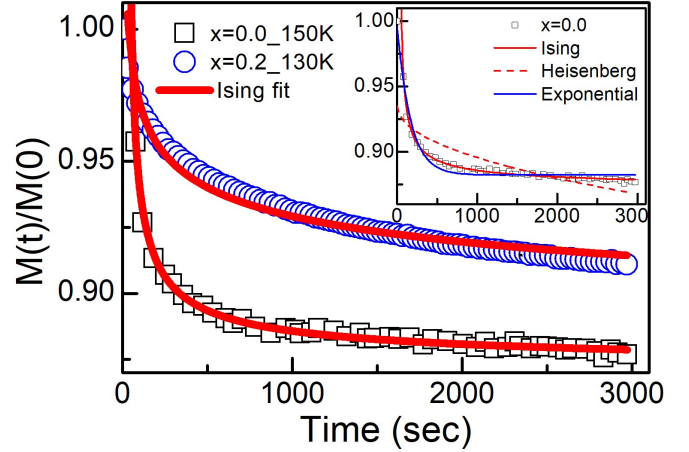


FIG. 9: Variation of normalized IRM with time decay measured at $T_C < T < T^*$ for the $x = 0.0$ (150 K) and $x = 0.2$ (130 K) samples, fitted with Ising model. Inset shows fitting at 150 K of $x = 0.0$ sample along with their Ising, Heisenberg and exponential model.

characteristic of YICO.

Figure 8a,b show the thermoremanent magnetization (TRM) of $x = 0.0$, 0.2 samples measured at different field. Sample was cooled down to low temperature in presence of applied field. After 10 sec waiting time, M vs T curve is measured in a heating cycle after sudden removal of field. Being a zero field measurement, TRM is likely to be advantageous in comparison with the traditional in-field χ_{dc} vs T measurements in identification of the GP singularity as the paramagnetic contribution to the magnetization is likely to be suppressed. Around T_{irr} the TRM exhibits a sharp upturn, while a sharp and sudden downturn in M_{TRM}^{-1} vs T curves [insets of Fig. 8] indicate the formation of rare regions at $T_C < T < T^*$.

In order to find the presence of magnetically ordered rare regions, isothermal remanent magnetization (IRM) at $T_C < T < T^*$ is carried out. In PM regime, IRM generally fall exponentially with time, while in GP regime, IRM fall non-exponentially with time because magnetically ordered rare regions would take larger time to reverse its effective spin^{2,3}. Long back, it have been proposed that in the GP regime, spin auto-correlation function $C(t)$ has to be the form of $C(t) \sim \exp[-A \ln(t)^{d/(d-1)}]$ for Ising system and $C(t) \sim \exp[-Bt^{1/2}]$ for Heisenberg system^{2,3}. Figure 9 shows the

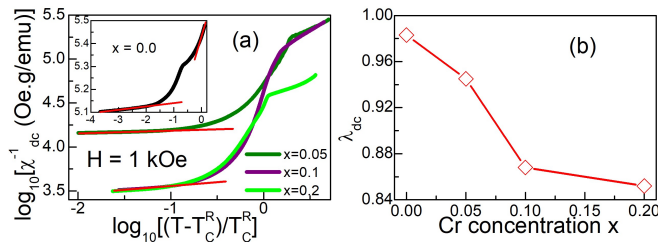


FIG. 10: (a) The temperature dependent susceptibility data, plotted in log-log scale. For clarity, $x = 0.0$ sample is shown in inset. (b) Dependence of the GP parameters with doping.

normalized IRM as a function of time for the two representative samples $x = 0.0$ (150 K), 0.2 (130 K). For the IRM measurement, the samples were cooled from 300 K to desired temperature in the presence of field 1 kOe. After stabilizing the temperature and waiting time up to 100 sec, variation of magnetization as a function of time (M vs. t) was measured after immediate removal of the field. Interestingly, IRM data indicate the best fit with the Ising spin model decay scheme [Fig. 9]. It shows the lack of agreement with the Heisenberg-like interactions as well as exponential decay model scheme [$M(t) = M(0) + A \exp(-\frac{t}{\tau})$] as shown in the inset of Fig. 9. It suggests that instead of PM state above T_C , system is in magnetically ordered rare region (which slows down the dynamics of spins). The observation of *Ising-like* interaction is consistent with prior reports, where the nature of spin correlation in the pyrochlore iridates was inferred to be Ising-like⁴⁹.

One of the standard methods to characterize the GP behaviour is to verify the $\frac{1}{\chi}$ vs T defined by $\chi^{-1} = (T - T_C^{Rand})^{1-\lambda}$, where, the exponent λ is positive but less than unity. Here T_C^{Rand} is the critical temperature of random FM clusters lying above T_C but below T^* . The exact estimation of T_C^{Rand} is a serious issue. An appropriate choice should be $T_C^{Rand} = \theta_{CW}$ so that efficiently it gives rise to $\lambda \sim 0$ in the PM region^{7,12,13}. The value of θ_{CW} is much lower than T_C . So, we approximately choose $T_C^{Rand} = T_C$. Figure 10a shows $\log_{10}(\chi^{-1})$ vs $\log_{10}(\frac{T - T_C^{Rand}}{T_C^{Rand}})$ plots. Fitting of the linear regime according to GP equation gives non-zero values of λ ranging between $0 \leq \lambda \leq 1$. The value of λ decreases systematically against Cr doping concentration [Fig. 10b]. We further estimate the value of normalized range of $GP_{Norm} = (\frac{T^* - T_C}{T_C})^{7.11}$ are given in Table I. The estimated value of GP_{Norm} is greater in substituted sample (1 order) as compared to $x = 0.0$ sample. Moreover, YICO series is showing significant enhancement in the value of GP_{Norm} compared to other systems^{9-11,13}.

Further, we look into the possible macroscopic origin of the formation of magnetically ordered rare regions. In parent compound Ir -site creates local disorder in the pyrochlore crystal structure with the doping of Cr -ion as reported by the same authors^{26,27}. As un-doped compound is a disordered sys-

tem exhibiting strong distorted cubic structure, the quenched disorder (a prerequisite of the GP) is inherent in the system. There are several reports on GP, which emerged due to B -site^{7,15,50} disorder with mixed oxidation states of transition metal ions. Distortion leads to the coexistence of mixed valence states of Ir , i.e. Ir^{4+} and Ir^{5+} in YICO series. Now, the random distribution of vacancies at Ir^{4+} -site locally reduces the $Ir^{4+} - Ir^{4+}$ interionic bond length where short range correlations are prevalent. It leads to the coexistence of two phases within the same crystalline state consistent with other systems exhibiting geometrically frustrated AFM spin arrangement¹¹⁻¹³.

IV. CONCLUSIONS

We investigate the experimental evidence of GP-like behaviour at $T_C < T < T^*$ in the Cr doped geometrically frustrated antiferromagnetic pyrochlore iridates $Y_2Ir_2O_7$. In a nutshell, the important observations are as follows:- (1) Hysteresis in M vs H curve, cusp in χ_{ZFC} vs T data at lower temperature than irreversible temperature T_{irr} , and relaxation in M vs time curve suggest cluster-glass-like state in YICO series, (2) Larger value of μ_{eff}^{exp} than μ_{eff}^{theo} , suggests the formation GP-like FM clusters, (3) Sudden and sharp downward deviation in $\frac{1}{\chi}$ vs T curves from conventional CW behaviour below T^* , a temperature much above the long range ordering temperature T_C , suggests formation magnetically ordered clusters, (4) The $\frac{1}{\chi}$ vs T curves measured at all applied magnetic field do not coincide on to a single curve above T^* in the true PM regime, (5) The lesser value of power exponent n than ideal value of 2 (for paramagnetic regime) at $T_C < T < T^*$ in $-\Delta S_M$ vs H curve, suggests presence of magnetic clusters, and (6) Slow dynamics of spin in IRM data at $T_C < T < T^*$ exhibiting Ising like interaction, favours the presence of magnetically ordered rare regions. Interestingly, all experimental observations suggests the presence of magnetically ordered rare regions in global paramagnetic matrix ranging $T_C < T < T^*$, favours GP-like state in YIO. The strength of magnetically ordered rare regions enhances with the substitution of Cr . Rare regions are distributed over a wide temperature regime. It is the first study of the GP along with cluster-glass-like states in the geometrically frustrated antiferromagnetic pyrochlore oxide family. The current finding is important and justify its importance among the rare materials which exhibit GP along with glass like states in AFM ordered systems, which is very limited till date.

V. ACKNOWLEDGMENTS

V. K. Dwivedi thanks Prof. Soumik Mukhopadhyay (IIT Kanpur) for his guidance during this project.

* Electronic address: vinodd.iitbombay@gmail.com

¹ K. Binder and A. P. Young, Spin glasses: Experimental facts, the-

- oretical concepts, and open questions, *Rev. Mod. Phys.* **58**, 801 (1986).
- ² M. Randeria, J. P. Sethna, and R. G. Palmer, Low-Frequency Relaxation in Ising Spin-Glasses, *Phys. Rev. Lett.* **54**, 1321 (1985).
 - ³ A. J. Bray, Nature of the Griffiths phase, *Phys. Rev. Lett.* **59**, 586 (1987).
 - ⁴ R. B. Griffiths, Nonanalytic Behavior Above the Critical Point in a Random Ising Ferromagnet, *Phys. Rev. Lett.* **23**, 17 (1969).
 - ⁵ J. Deisenhofer, D. Braak, H.-A. K. v. Nidda, J. Hemberger, R. M. Eremina, V. A. Ivanshin, A. M. Balbashov, G. Jug, A. Loidl, T. Kimura, and Y. Tokura, Observation of a Griffiths Phase in Paramagnetic $La_{1-x}Sr_xMnO_3$, *Phys. Rev. Lett.* **95**, 257202 (2005).
 - ⁶ M. B. Salamon, P. Lin, and S. H. Chun, Colossal Magnetoresistance is a Griffiths Singularity, *Phys. Rev. Lett.* **88**, 197203 (2002).
 - ⁷ A. K. Pramanik and A. Banerjee, Griffiths phase and its evolution with Mn-site disorder in the half-doped manganite $Pr_{0.5}Sr_{0.5}Mn_{1-y}Ga_yO_3$ ($y = 0.0, 0.025, \text{ and } 0.05$), *Phys. Rev. B* **81**, 024431 (2010).
 - ⁸ V. K. Shukla and S. Mukhopadhyay, Antiferromagnetic rare region effect in $Pr_{0.5}Ca_{0.5}MnO_3$, *Phys. Rev. B* **97**, 054421 (2018).
 - ⁹ V. K. Dwivedi, and S. Mukhopadhyay, Suppression of long range magnetic ordering and electrical conduction in $Y_{1.7}Bi_{0.3}Ir_2O_7$ thin film, *J. Magn. Magn. Mater* **484**, 313 (2019). Evolution of structural, magnetic and electrical transport properties of $Y_{1.7}Bi_{0.3}Ir_2O_7$ thin film grown on YSZ(100) substrate by PLD, *Physica B: Condens. Matter* **571**, 137 (2019).
 - ¹⁰ C. Magen, P. A. Algarabel, L. Morellon, J. P. Araújo, C. Ritter, M. R. Ibarra, A. M. Pereira, and J. B. Sousa, Observation of a Griffiths-like Phase in the Magnetocaloric Compound $Tb_5Si_2Ge_2$, *Phys. Rev. Lett.* **96**, 167201 (2006).
 - ¹¹ Z. W. Ouyang, N. M. Xia, Y. Y. Wu, S. S. Sheng, J. Chen, Z. C. Xia, L. Li, and G. H. Rao, Short-range ferromagnetic correlations in the spin-chain compound Ca_3CoMnO_6 , *Phys. Rev. B* **84**, 054435 (2011).
 - ¹² J. Kumar, S. N. Panja, S. Dengre, and S. Nair, Identification of a Griffiths singularity in a geometrically frustrated antiferromagnet, *Phys. Rev. B* **95**, 054401 (2017).
 - ¹³ K. Ghosh, C. Mazumdar, R. Ranganathan, and S. Mukherjee, Griffiths phase behaviour in a frustrated antiferromagnetic intermetallic compound, *Sci. Rep.* **5**, 15801 (2015).
 - ¹⁴ E. V. Sampathkumaran, N. Mohapatra, S. Rayaprol, and K. K. Iyer, Magnetic anomalies in the spin-chain compound Sr_3CuRhO_6 : Griffiths-phase-like behavior of magnetic susceptibility, *Phys. Rev. B* **75**, 052412 (2007).
 - ¹⁵ A. Pal, P. Singh, V. K. Gangwar, S. Ghosh, P. Prakash, S. K. Saha, A. Das, M. Kumar, A. K. Ghosh, and S. Chatterjee, B-site disorder driven multiple-magnetic phases: Griffiths phase, re-entrant cluster glass, and exchange bias in Pr_2CoFeO_6 , *Appl. Phys. Lett.* **114**, 252403 (2019).
 - ¹⁶ W. W.-Krempa, G. Chen, Y. B. Kim, and L. Balents, Correlated Quantum Phenomena in the Strong Spin-Orbit Regime, *Annu. Rev. Condens. Matter Phys.* **5**, 57 (2014).
 - ¹⁷ X. Wan, A. M. Turner, A. Vishwanath, and S. Y. Savrasov, Topological semimetal and Fermi-arc surface states in the electronic structure of pyrochlore iridates, *Phys. Rev. B* **83**, 205101 (2011).
 - ¹⁸ A. Juyal, A. Agarwal, and S. Mukhopadhyay, Evidence of density waves in single-crystalline nanowires of pyrochlore iridates, *Phys. Rev. B* **95**, 125436 (2017). Negative Longitudinal Magnetoresistance in the Density Wave Phase of $Y_2Ir_2O_7$, *Phys. Rev. Lett.* **120**, 096801 (2018).
 - ¹⁹ N. Aito, M. Soda, Y. Kobayashi and M. Sato, Spin-Glass-like Transition and Hall Resistivity of $Y_{2-x}Bi_xIr_2O_7$, *J. Phys. Soc. Jpn.* **72**, 1226 (2003).
 - ²⁰ N. Taira, M. Wakeshima, and Y. Hinatsu, Magnetic properties of iridium pyrochlores $R_2Ir_2O_7$ ($R = Y, Sm, Eu \text{ and } Lu$), *J. Phys.: Condens. Matter* **13**, 5527 (2001).
 - ²¹ W. K. Zhu, M. Wang, B. Seradjeh, F. Yang, and S. X. Zhang, Enhanced weak ferromagnetism and conductivity in hole-doped pyrochlore iridate $Y_2Ir_2O_7$, *Phys. Rev. B* **90**, 054419 (2014).
 - ²² B. Ghosh, V. K. Dwivedi, and S. Mukhopadhyay, Non-Fermi liquid regime in metallic pyrochlore iridates: Quantum Griffiths singularities, *Phys. Rev. B* **102**, 144444 (2020).
 - ²³ H. Kumar, R. S. Dhaka, and A. K. Pramanik, Evolution of structure, magnetism, and electronic transport in the doped pyrochlore iridate $Y_2Ir_{2-x}Ru_xO_7$, *Phys. Rev. B* **95**, 054415 (2017).
 - ²⁴ H. Kumar, and A. K. Pramanik, Nonmagnetic Substitution in Pyrochlore Iridate $Y_2(Ir_{1-x}Ti_x)_2O_7$: Structure, Magnetism, and Electronic Properties, *J. Phys. Chem. C* **123**, 13036 (2019).
 - ²⁵ H. Kumar, K. C. Kharkwal, K. Kumar, K. Asokan, A. Banerjee, and A. K. Pramanik, Magnetic and transport properties of the pyrochlore iridates $(Y_{1-x}Pr_x)_2Ir_2O_7$: Role of f d exchange interaction and d p orbital hybridization, *Phys. Rev. B* **101**, 064405 (2020).
 - ²⁶ V. K. Dwivedi, and S. Mukhopadhyay, Coexistence of high electrical conductivity and weak ferromagnetism in Cr doped $Y_2Ir_2O_7$ pyrochlore iridates, *J. Appl. Phys.* **125**, 223901 (2019).
 - ²⁷ V. K. Dwivedi, P. Mandal, and S. Mukhopadhyay, Frustration induced inversion of magnetocaloric effect and metamagnetic transition in substituted pyrochlore iridates, *ACS Appl. Electron. Mater.* **4**, 1611 (2022). Frustration induced inversion of magnetocaloric effect and enhanced cooling power in substituted Pyrochlore Iridates, [arXiv.2110.03570](https://arxiv.org/abs/2110.03570), (2021).
 - ²⁸ V. K. Dwivedi, and S. Mukhopadhyay, Influence of electronic structure parameters on the electrical transport and magnetic properties of $Y_{2-x}Bi_xIr_2O_7$ pyrochlore iridates, *J. Appl. Phys.* **126**, 165112 (2019).
 - ²⁹ H. Liu, J. Bian, S. Chen, J. Wang, Y. Feng, W. Tong, Y. Xie, B. Fang, Evolution of magnetism and electrical properties in the doped pyrochlore iridate $Y_2Ir_{2-x}Fe_xO_7$, *J. Magn. Magn. Mater* **498**, 166214 (2020).
 - ³⁰ H. Liu, J. Bian, S. Chen, Y. Wang, Y. Feng, W. Tong, Y. Xie, B. Fang, Enhanced ferromagnetism and Mott variable-range hopping behavior in Cu doped pyrochlore iridate $Y_2Ir_2O_7$, *Physica B: Condensed Matter* **568**, 60 (2019).
 - ³¹ A. Juyal, V. K. Dwivedi, S. Verma, S. Nandi, A. Agarwal, and S. Mukhopadhyay, Possible transition between charge density wave and Weyl semimetal phase in $Y_2Ir_2O_7$, *Phys. Rev. B* **106**, 155149 (2022). Charge density wave and Weyl Semimetal phase in $Y_2Ir_2O_7$, [arXiv.2206.00690](https://arxiv.org/abs/2206.00690), (2022).
 - ³² V. K. Dwivedi, A. Juyal, and S. Mukhopadhyay, Colossal enhancement of electrical conductivity in $Y_2Ir_2O_7$ nanoparticles, *Mater. Res. Express* **3**, 115020 (2016). Structural and magnetic studies of nanocrystalline $Y_2Ir_2O_7$, *AIP Conf. Proc.* **1665**, 050160 (2015).
 - ³³ D. Lebedev, M. Povia, K. Waltar, P. M. Abdala, I. E. Castelli, E. Fabbri, M. V. Blanco, A. Fedorov, C. Coperet, N. Marzari, and T. J. Schmidt, Highly Active and Stable Iridium Pyrochlores for Oxygen Evolution Reaction, *Chem. Mater.* **29**, 5182 (2017).
 - ³⁴ P.-C. Shih, Jaemin Kim, C.-J. Sun, and H. Yang, Single-Phase Pyrochlore $Y_2Ir_2O_7$ Electrocatalyst on the Activity of Oxygen Evolution Reaction, *ACS Appl. Energy Mater* **1**, 3992 (2018).
 - ³⁵ M. A. Hubert, A. Gallo, Y. Liu, E. Valle, J. Sanchez, D. Sokaras, R. Sinclair, L. A. King, and T. F. Jaramillo, Characterization of a Dynamic $Y_2Ir_2O_7$ Catalyst during the Oxygen Evolution Reaction in Acid, *J. Phys. Chem. C* **126**, 1751 (2022).
 - ³⁶ X. Liu, F. Wen, E. Karapetrova, J.-W. Kim, P. J. Ryan, J. W. Freeland, M. Terilli, T.-C. Wu, M. Kareev, and J. Chakhalian, *In-situ*

- fabrication and transport properties of (111) $Y_2Ir_2O_7$ epitaxial thin film, *Appl. Phys. Lett.* **117**, 041903 (2020).
- ³⁷ M. C. Shapiro, S. C. Riggs, M. B. Stone, C. R. d. l. Cruz, S. Chi, A. A. Podlesnyak, and I. R. Fisher, Structure and magnetic properties of the pyrochlore iridate $Y_2Ir_2O_7$, *Phys. Rev. B* **85**, 214434 (2012).
- ³⁸ S. M. Disseler, C. Dhital, A. Amato, S. R. Giblin, C. d. l. Cruz, S. D. Wilson, and M. J. Graf, Magnetic order in the pyrochlore iridates $A_2Ir_2O_7$ ($A = Y, Yb$), *Phys. Rev. B* **86**, 014428 (2012).
- ³⁹ S. M. Disseler, Direct evidence for the all-in/all-out magnetic structure in the pyrochlore iridates from muon spin relaxation, *Phys. Rev. B* **89**, 140413(R) (2014).
- ⁴⁰ T. M. Fernandez, Magnetic characterization of $Y_{2-x}Bi_xIr_2O_7$: A muon spin rotation/relaxation and susceptibility study, *M. Sc. Thesis, McMaster University*, (2014).
- ⁴¹ A. Julia, Muon-spin relaxation study of Ir-spin fluctuations in hole-doped pyrochlore iridates $(Y_{1-x-y}Cu_xCa_y)_2Ir_2O_7$, *Ph. D. Thesis, Hokkaido University*, (2019).
- ⁴² H. Kumar, and A. K. Pramanik, Nonequilibrium low temperature phase in pyrochlore iridate $Y_2Ir_2O_7$: Possibility of glass-like dynamics, *J. Magn. Magn. Mater* **409**, 20 (2016).
- ⁴³ H. Liu, W. Tong, L. Ling, S. Zhang, R. Zhang, L. Zhang, L. Pi, C. Zhang, Y. Zhang, Magnetic order, spin dynamics and transport properties of the pyrochlore iridate $Y_2Ir_2O_7$, *Solid State Commun.* **179**, 1 (2014).
- ⁴⁴ V. K. Dwivedi, and S. Mukhopadhyay, Effect of stoichiometry on magnetic and transport properties in polycrystalline $Y_2Ir_2O_7$, *AIP Conf. Proc.* **1953**, 120002 (2018). Study of optical properties of polycrystalline $Y_2Ir_2O_7$, *AIP Conf. Proc.* **1832**, 090016 (2017).
- ⁴⁵ Y. M. Liang, Z. J. Wang, Y. Bai, Y. J. Wu, X. K. Ning, X. F. Xiao, X. G. Zhao, W. Liu, and Z. D. Zhang, Interface-induced transition from a cluster glass state to a spin glass state in $LaMnO_3/BiFeO_3$ heterostructures, *J. Mater. Chem. C* **7**, 2376 (2019).
- ⁴⁶ C. He, M. A. Torija, J. Wu, J. W. Lynn, H. Zheng, J. F. Mitchell, and C. Leighton, Non-Griffiths-like clustered phase above the Curie temperature of the doped perovskite cobaltite $La_{1-x}Sr_xCoO_3$, *Phys. Rev. B* **76**, 014401 (2007).
- ⁴⁷ M. M. Saber, M. Egilmez, A. I. Mansour, I. Fan, K. H. Chow, and J. Jung, Evolution of Curie-Weiss behavior and cluster formation temperatures in Ru-doped $Sm_{0.55}Sr_{0.45}MnO_3$ manganites, *Phys. Rev. B* **82**, 172401 (2010).
- ⁴⁸ A. Kumar, and R. S. Dhaka, Unraveling magnetic interactions and the spin state in insulating $Sr_{2-x}La_xCoNbO_6$, *Phys. Rev. B* **101**, 094434 (2020).
- ⁴⁹ L. Savary, E.-G. Moon, and L. Balents, New Type of Quantum Criticality in the Pyrochlore Iridates, *Phys. Rev. X* **4**, 041027 (2014).
- ⁵⁰ R. S. Silva, Jr., C. Santos, M. T. Escote, B. F. O. Costa, N. O. Moreno, S. P. A. Paz, R. S. Angélica, and N. S. Ferreira, Griffiths-like phase, large magnetocaloric effect, and unconventional critical behavior in the $NdSrCoFeO_6$ disordered double perovskite, *Phys. Rev. B* **106**, 134439 (2022).